AAS 21-369

A NEW METHODOLOGY FOR THE SOLUTION OF THE STIFFNESS PROBLEM APPLIED TO LOW-THRUST TRAJECTORY OPTIMISATION IN TERMS OF ORBITAL ELEMENTS USING DIFFERENTIAL DYNAMIC PROGRAMMING

Marco Nugnes,[*] and Camilla Colombo[†]

The largest part of direct and indirect methods for trajectory optimisation exploits Cartesian coordinates as state representation of the dynamical systems. However, for specific dynamical systems such as orbit dynamics, orbital elements represent an attractive alternative because they provide a physical insight into the time evolution of the orbit geometry. The use of the orbital elements though makes the dynamical system stiff because of the different time evolution between fast and slow variables. This paper proposes a solution to the stiffness problem for the low-thrust trajectory optimisation using orbital elements as state representation and the Differential Dynamics Programming as optimization method.

INTRODUCTION

Low-thrust trajectory optimization represents one of the classic nonlinear constrained optimal control problems in the field of space applications. The interest in such problems is related to the increase in the development of all-electric spacecraft in the design of current and future space missions because they grant a low fuel mass consumption thanks to their high specific impulse.

The largest part of direct and indirect methods used for the solution of a generic dynamical system involves a Cartesian representation for the dynamics. However, for some specific problems such as orbital dynamics, there are other state representations which are a valid alternative to the Cartesian coordinates. In fact, the solution of an orbital dynamics problem in terms of Cartesian coordinates provides no physical insight about the orbit geometry (e.g., orbit shape, orbital plane inclination) until the three-dimensional trajectory is plotted. Moreover, no information about the time evolution of the orbital trajectory is given. Orbital elements are defined starting from the orbit geometry in 3D space and they are associated to the orbital mechanics integral of motions such as the total energy, the angular momentum and the eccentricity. This is the reason why they should be preferred in place of the classic Cartesian representation for the solution of space trajectories.

The largest part of the works about low-thrust trajectory optimization problem in terms of orbital elements involves semi-analytical theories, phase space representations, classic di-

[*] PhD Candidate, Department of Aerospace Science and Technology, Politecnico di Milano, marco.nugnes@polimi.it.
[†] Associate Professor, Department of Aerospace Science and Technology, Politecnico di Milano, camilla.colombo@polimi.it.

rect/indirect methods.[1,2] In this paper the Differential Dynamic Programming (DDP) technique is used. The first complete definition of this technique has been provided by Jacobson and Mayne focusing on the continuous version of the algorithm.[3] Gershwin and Jacobson extended the DDP also for discrete optimal control problems.[4] The DDP optimization algorithm has been used not only for space applications, but also in other fields such as the determination of multi-reservoir system control and feedback control of groundwater remediation.[5,6] Starting from the DDP, Whiffen developed the Mystic software that was used for the first time in the design of NASA's cancelled Jupiter Icy Moon Orbiter (JIMO) mission's reference trajectory.[7] The original version of the algorithm has been modified by Colombo et al. introducing an adaptive numerical scheme for the application of the DDP to low-thrust trajectory optimisation problem.[8] Lantoine and Russel developed a Hybrid Differential Dynamics Programming (HDDP) based on the use of the State Transition Matrix (STM) for the computation of the partials to be provided to the optimization algorithm.[9] Finally, Ozaki et al. described a Stochastic Differential Dynamic Programming (SDDP) to extend the application of this method not only to deterministic problems.[10] In all these works, the formulation of the dynamics for the DDP technique is always in Cartesian coordinates and there is no attempt to couple the DDP with the orbital elements as state representation.

In this paper the DDP optimisation algorithm is used coupled with orbital elements as state representation. The dynamics of the orbital motion is described using Gauss' variational equations. The complete description of the convergence problems arising from the application of angular variables and the respective solutions are provided. Finally, the DDP algorithm is applied to a Mars interplanetary transfer, near-Earth asteroid transfer, and Earth-satellite orbit raising to verify the effectiveness of the algorithm with the orbital elements.

MODELLING

In this section a summary about the derivation of the DDP optimisation algorithm is presented together with the assumptions used to get the results.

Differential Dynamic Programming

The DDP is an optimisation algorithm for solving nonlinear optimal control problems. It is based on Bellman's principle of optimality that can be mathematically represented using Hamilton-Jacobi-Bellman (HJB) equations in its continuous version:

$$\frac{\partial V(\mathbf{x},t)}{\partial t} = -\min_{\mathbf{u}(t)}\left[J(\mathbf{x},\mathbf{u},t) + \mathbf{f}(\mathbf{x},\mathbf{u},t)\cdot\nabla V(\mathbf{x},t)\right] \tag{1}$$

where V is the value function, J is the functional cost and $\mathbf{f}$ represents the equations of motion describing the dynamics of the system. The HJB equation is a partial differential equation which does not admit an analytical solution. However, no numerical solution can be likewise obtained because the search space is made up of functions and it has no finite dimension. This is defined in literature as the "curse of dimensionality".[11] The DDP represents a linear-quadratic expansion of HJB equation starting from a nonoptimal solution used as first guess. This way it is possible to apply Bellman's principle of optimality to obtain at least a local optimal solution, because the global optimality is lost due to the application of the linear-quadratic expansion. The HJB equation also admits a discrete version that can be coupled with the numerical integration schemes:

$$V_k^*(\mathbf{x}_k,\mathbf{b}_k,t_k) = \min_{\mathbf{u}_k}\left[J_k(\mathbf{x}_k,\mathbf{u}_k,t_k) + V_{k+1}^*(\mathbf{x}_{k+1},\mathbf{b}_k,t_{k+1})\right] \tag{2}$$

where V^*_{k+1} represents the optimal value function obtained at the successive step t_{k+1}, and $\mathbf{b}_k$ is the vector of Lagrange multipliers used to adjoint the endpoint constraints to the cost function, J, for the definition of the value function, V. In this work the discrete version of the DDP algorithm is used. The arguments of the function in Eq. (2) can be formulated as the sum of a nominal initial guess and a small variation in the following way:

$$\mathbf{x}_k = \bar{\mathbf{x}}_k + \delta\mathbf{x}_k, \quad \mathbf{u}_k = \bar{\mathbf{u}}_k + \delta\mathbf{u}_k, \quad \mathbf{x}_{k+1} = \bar{\mathbf{x}}_{k+1} + \delta\mathbf{x}_{k+1}, \quad \mathbf{b}_k = \bar{\mathbf{b}}_k + \delta\mathbf{b}_k \tag{3}$$

$$V_k^*\left(\bar{\mathbf{x}}_k + \delta\mathbf{x}_k, \bar{\mathbf{b}}_k + \delta\mathbf{b}_k\right) = \min_{\delta\mathbf{u}_k}\left[J_k\left(\bar{\mathbf{x}}_k + \delta\mathbf{x}_k, \bar{\mathbf{u}}_k + \delta\mathbf{u}_k\right) + V_{k+1}^*\left(\bar{\mathbf{x}}_{k+1} + \delta\mathbf{x}_{k+1}, \bar{\mathbf{b}}_k + \delta\mathbf{b}_k\right)\right]. \tag{4}$$

Each term is expanded in Taylor series starting from the initial nominal guess stopping at the second-order term to be consistent with the linear-quadratic expansion assumption. The expansions related to the optimal value function and functional cost are reported:

$$\begin{aligned} V_k^*\left(\bar{\mathbf{x}}_k + \delta\mathbf{x}_k, \bar{\mathbf{b}}_k + \delta\mathbf{b}_k, t_k + \delta t_k\right) &= V_k\left(\bar{\mathbf{x}}_k, \bar{\mathbf{b}}_k, t_k\right) + \left[V_x^k\left(\bar{\mathbf{x}}_k, b_k, t_k\right)\right]^T \delta\mathbf{x}_k + \\ &+ \left[V_b^k\left(\bar{\mathbf{x}}_k, \bar{\mathbf{b}}_k, t_k\right)\right]^T \delta\mathbf{b}_k + \frac{1}{2}\delta\mathbf{x}_k^T V_{xx}^k\left(\bar{\mathbf{x}}_k, \bar{\mathbf{b}}_k, t_k\right)\delta\mathbf{x}_k + \frac{1}{2}\delta\mathbf{b}_k^T V_{bb}^k\left(\bar{\mathbf{x}}_k, \bar{\mathbf{b}}_k, t_k\right)\delta\mathbf{b}_k + \\ &+ \delta\mathbf{x}_k^T V_{xb}^k\left(\bar{\mathbf{x}}_k, \bar{\mathbf{b}}_k, t_k\right)\delta\mathbf{b}_k \end{aligned} \tag{5}$$

$$\begin{aligned} L_k\left(\bar{\mathbf{x}}_k + \delta\mathbf{x}_k, \bar{\mathbf{u}}_k + \delta\mathbf{u}_k, t_k + \delta t_k\right) &= L_k\left(\bar{\mathbf{x}}_k, \bar{\mathbf{u}}_k, t_k\right) + \left[L_x^k\left(\bar{\mathbf{x}}_k, \bar{\mathbf{u}}_k, t_k\right)\right]^T \delta\mathbf{x}_k + \\ &+ \left[L_u^k\left(\bar{\mathbf{x}}_k, \bar{\mathbf{u}}_k, t_k\right)\right]^T \delta\mathbf{u}_k + \frac{1}{2}\delta\mathbf{x}_k^T L_{xx}^k\left(\bar{\mathbf{x}}_k, \bar{\mathbf{u}}_k, t_k\right)\delta\mathbf{x}_k + \frac{1}{2}\delta\mathbf{u}_k^T L_{uu}^k\left(\bar{\mathbf{x}}_k, \bar{\mathbf{u}}_k, t_k\right)\delta\mathbf{u}_k + \\ &+ \delta\mathbf{x}_k^T L_{xu}^k\left(\bar{\mathbf{x}}_k, \bar{\mathbf{u}}_k, t_k\right)\delta\mathbf{u}_k \end{aligned} \tag{6}$$

$$\begin{aligned} V_{k+1}^*\left(\bar{\mathbf{x}}_{k+1} + \delta\mathbf{x}_{k+1}, \bar{\mathbf{b}}_k + \delta\mathbf{b}_k\right) &= V_{k+1}\left(\bar{\mathbf{x}}_{k+1}, \bar{\mathbf{b}}_k\right) + \left[V_x^{k+1}\left(\bar{\mathbf{x}}_{k+1}, b_k\right)\right]^T \delta\mathbf{x}_{k+1} + \\ &+ \left[V_b^{k+1}\left(\bar{\mathbf{x}}_{k+1}, \bar{\mathbf{b}}_k\right)\right]^T \delta\mathbf{b}_k + \frac{1}{2}\delta\mathbf{x}_{k+1}^T V_{xx}^{k+1}\left(\bar{\mathbf{x}}_{k+1}, \bar{\mathbf{b}}_k\right)\delta\mathbf{x}_{k+1} + \\ &+ \frac{1}{2}\delta\mathbf{b}_k^T V_{bb}^{k+1}\left(\bar{\mathbf{x}}_{k+1}, \bar{\mathbf{b}}_k\right)\delta\mathbf{b}_k + \delta\mathbf{x}_{k+1}^T V_{xb}^{k+1}\left(\bar{\mathbf{x}}_{k+1}, \bar{\mathbf{b}}_k\right)\delta\mathbf{b}_k \end{aligned} \tag{7}$$

At this point the algorithm can be formulated in its “local” or “global” version:

- the local version keeps the nominal trajectory as starting point of the expansions.
- the global version uses as initial guess for the expansions the optimal control $\mathbf{u}^*$ obtained from Eq. (4) with all the variations equal to zero.

The difference between the two versions of the DDP algorithm is in the magnitude of the control variations. Being the starting point of the expansions in the “global” version coming from an optimisation problem, the search space for the overall optimal control problem is increased.

All the expansions are replaced in the HJB equation and the new task is to determine the optimal control variation that minimizes the quantity inside the square brackets. The evaluation of the optimal solution is carried out thanks to the differentiation with respect to the control variation leading to a linear feedback control law.

$$\delta\mathbf{u}_k = \beta\delta\mathbf{x}_k + \gamma\delta\mathbf{b}_k \tag{8}$$

Replacing the feedback control law in the expanded HJB equation a set of backward difference equations is obtained equating the coefficients multiplying the same partials. The initial condition for the backward difference equations is given by the final state. The DDP can be summarised as a technique that is divided in a first backward sweep where the optimal control feedback law is computed and a second forward integration where the control law is applied. The process goes on until no further minimisation is obtained.

Dynamics Formulation

One of the advantages in using the DDP algorithm is the parametrisation of the dynamics associated to the problem. This implies that it is possible to write the equations of motion in a script that is external to the optimisation algorithm. For orbital mechanics applications, the best formulation to express the orbit dynamics of a generic satellite is given by Gauss' and Lagrange planetary equations coupled with the mass rate equation that consider both conservative and non-conservative accelerations. In this work the formulation of Gauss' variational equations in the transversal-normal-orthogonal orbital frame $\left[\hat{\mathbf{t}},\hat{\mathbf{n}},\hat{\mathbf{h}}\right]$ is used:[12]

$$
\begin{aligned}
\frac{da}{dt} &= \frac{2a^2 v}{\mu}\frac{u_t}{m} \\
\frac{de}{dt} &= \frac{1}{v}\left[2\left(e+\cos f\right)\frac{u_t}{m} - \frac{r}{a}\sin f\,\frac{u_n}{m}\right] \\
\frac{di}{dt} &= \frac{r\cos\theta}{h}\frac{u_h}{m} \\
\frac{d\Omega}{dt} &= \frac{r\sin\theta}{h\sin i}\frac{u_h}{m} \\
\frac{d\omega}{dt} &= \frac{1}{ev}\left[2\sin f\,\frac{u_t}{m} + \left(2e+\frac{r}{a}\cos f\right)\frac{u_n}{m}\right] - \frac{r\sin\theta\cos i}{h\sin i}\frac{u_h}{m} \\
\frac{df}{dt} &= \frac{h}{r^2} - \frac{1}{ev}\left[2\sin f\,\frac{u_t}{m} + \left(2e+\frac{r}{a}\cos f\right)\frac{u_n}{m}\right] \\
\frac{dm}{dt} &= -\frac{1}{Isp\, g_0}\sqrt{u_t^2+u_n^2+u_h^2}
\end{aligned}
\tag{9}
$$

where a, e, i, Ω, ω, f are the osculating semi-major axis, eccentricity, inclination, Right Ascension of the Ascending Node (RAAN), pericentre anomaly, and true anomaly, respectively. The vector $[u_t, u_n, u_h]$ represent the components of the disturbing forces that are the sum of the control actions and the orbital perturbations while m id the mass of the satellite and I_{sp} the specific impulse.

The previous formulation of the dynamics is not in a good shape for numerical integration because of the difference in terms of order of magnitudes between the orbital parameters. Therefore, Gauss' equations are rewritten considering adimensional orbital elements and disturbing accelerations so that each variable can range between [0,1]. The following set of reference quantities has been used for the adimensionalisation process:

$$
\begin{aligned}
L_{ref} &= \begin{cases} a_i & if \quad a_i > a_f \\ a_f & if \quad a_i \le a_f \end{cases} \\
t_{ref} &= \sqrt{\frac{L_{ref}^3}{\mu}} \\
m_{ref} &= \frac{m_0}{n} \\
v_{ref} &= \sqrt{\frac{\mu}{L_{ref}}} \\
u_{ref} &= m_{ref}\,\frac{\mu}{L_{ref}^2}
\end{aligned} \tag{10}
$$

The n divisor used for definition of the reference mass is introduced to avoid that adimensional mass is close to zero leading to a divergence of the integration of the equations of motions. Using the reference quantities given by Eq. (10), Gauss' adimensional equations are formulated in the following manner:

$$
\begin{aligned}
\frac{d\tilde{a}}{d\tilde{t}} &= 2\sqrt{\frac{\tilde{a}^3}{1-e^2}\left(1+2e\cos f+e^2\right)}\,\frac{\tilde{u}_t}{\tilde{m}} \\
\frac{de}{d\tilde{t}} &= \sqrt{\frac{\tilde{a}\left(1-e^2\right)}{1+2e\cos f+e^2}}\left[2\left(e+\cos f\right)\frac{\tilde{u}_t}{\tilde{m}}-\frac{1-e^2}{1+e\cos f}\sin f\,\frac{\tilde{u}_n}{\tilde{m}}\right] \\
\frac{di}{d\tilde{t}} &= \sqrt{\tilde{a}\left(1-e^2\right)}\,\frac{\cos\left(\omega+f\right)}{1+e\cos f}\,\frac{\tilde{u}_h}{\tilde{m}} \\
\frac{d\Omega}{d\tilde{t}} &= \sqrt{\tilde{a}\left(1-e^2\right)}\,\frac{\sin\left(\omega+f\right)}{\sin i\left(1+e\cos f\right)}\,\frac{\tilde{u}_h}{\tilde{m}} \\
\frac{d\omega}{d\tilde{t}} &= \sqrt{\tilde{a}\left(1-e^2\right)}\left\{\frac{1}{e\sqrt{1+2e\cos f+e^2}}\left[2\sin f\,\frac{\tilde{u}_t}{\tilde{m}}+\frac{2e+\cos f+e^2\cos f}{1+e\cos f}\,\frac{\tilde{u}_n}{\tilde{m}}\right]+\right. \\
&\qquad \left.-\frac{\sin\left(\omega+f\right)}{1+e\cos f}\,\frac{\cos i}{\sin i}\,\frac{\tilde{u}_h}{\tilde{m}}\right\} \\
\frac{df}{d\tilde{t}} &= \frac{\left(1+e\cos f\right)^2}{\left[a\left(1-e^2\right)\right]^{\frac{3}{2}}}-\frac{1}{e}\sqrt{\frac{\tilde{a}\left(1-e^2\right)}{1+e\cos f+e^2}}\left[2\sin f\,\frac{\tilde{u}_t}{\tilde{m}}+\frac{2e+\cos f+e^2\cos f}{1+e\cos f}\,\frac{\tilde{u}_n}{\tilde{m}}\right] \\
\frac{d\tilde{m}}{d\tilde{t}} &= -\sqrt{\frac{\mu}{L_{ref}}}\,\frac{1}{Isp\;g_0}\sqrt{\tilde{u}_t^2+\tilde{u}_n^2+\tilde{u}_h^2}
\end{aligned} \tag{11}
$$

The previous formulation considers classic Keplerian elements as representation of the state. This introduces limitations on the orbits that can be considered because of the singularities related to the equations of motion. Gauss' variational equations in terms of classic Keplerian elements are singular for circular orbits ($e = 0$) and equatorial orbits ($i = 0$). Even if there are only two singularities, both circular orbits and equatorial orbits are of particular interest for space missions. It is necessary to introduce a set of non-singular elements to handle the previous two cases. In this work modified equinoctial elements have been considered for this purpose.[13] Gauss' variational equations can be rewritten in terms of modified equinoctial elements assuming the following form after the adimensionalisation process considering the same set of reference variables in the radial-transversal-orthogonal $\left[\hat{\mathbf{r}},\hat{\boldsymbol{\theta}},\hat{\mathbf{h}}\right]$ reference frame:

$$
\begin{aligned}
\frac{d\tilde{p}}{d\tilde{t}} &= 2\sqrt{\frac{\tilde{p}^3}{1+f\cos L+g\sin L}}\frac{\tilde{u}_\theta}{\tilde{m}} \\
\frac{df}{d\tilde{t}} &= \sqrt{\frac{\tilde{p}}{1+f\cos L+g\sin L}}\left\{\left(1+f\cos L+g\sin L\right)\sin L\frac{\tilde{u}_r}{\tilde{m}}+\left[f+\cos L\left(2+\right.\right.\right. \\
&\quad \left.\left.\left.+f\cos L+g\sin L\right]\frac{\tilde{u}_\theta}{\tilde{m}}-g\left(h\sin L-k\cos L\right)\frac{\tilde{u}_h}{\tilde{m}}\right\} \\
\frac{dg}{d\tilde{t}} &= \sqrt{\frac{p}{1+f\cos L+g\sin L}}\left\{-\left(1+f\cos L+g\sin L\right)\cos L\frac{\tilde{u}_r}{\tilde{m}}+\left[g+\sin L\left(2+\right.\right.\right. \\
&\quad \left.\left.\left.+f\cos L+g\sin L\right]\frac{\tilde{u}_\theta}{\tilde{m}}+f\left(h\sin L-k\cos L\right)\frac{\tilde{u}_h}{\tilde{m}}\right\} \\
\frac{dh}{d\tilde{t}} &= \frac{\sqrt{\tilde{p}}}{2}\frac{\left(1+h^2+k^2\right)}{1+f\cos L+g\sin L}\cos L\frac{\tilde{u}_h}{\tilde{m}} \\
\frac{dk}{d\tilde{t}} &= \frac{\sqrt{\tilde{p}}}{2}\frac{\left(1+h^2+k^2\right)}{1+f\cos L+g\sin L}\sin L\frac{\tilde{u}_h}{\tilde{m}} \\
\frac{dL}{d\tilde{t}} &= \frac{\left(1+f\cos L+g\sin L\right)^2}{\tilde{p}^{\frac{3}{2}}}+\frac{\sqrt{\tilde{p}}}{1+f\cos L+g\sin L}\left(h\sin L-k\cos L\right)\frac{\tilde{u}_h}{\tilde{m}} \\
\frac{d\tilde{m}}{d\tilde{t}} &= -\sqrt{\frac{\mu}{L_{ref}}}\frac{1}{Isp\ g_0}\sqrt{\tilde{u}_r^2+\tilde{u}_\theta^2+\tilde{u}_h^2}
\end{aligned}
\tag{12}
$$

Constrained Formulation

Another important aspect in the definition of the nonlinear control problem is given by the formulation used for the endpoint constraints. The constraints are adjoint with the cost function using Lagrange multipliers creating the final value function used in the derivation of the DDP algorithm. Therefore, the partials computation and the Lagrange multipliers' initial guess depend on the analytical formulation of the endpoint constraints.

In this paper, the endpoint constraints have been expressed using a quadratic formulation. This ensures that that the value function is always positive, and the minimisation process translates in the reduction of the cost towards zero.

$$\boldsymbol{\varphi}\left(\mathbf{x}_f, t_f\right)=\begin{cases}\left[\tilde{a}\left(t_f\right)-\tilde{a}_f\right]^2 \\ \left[e\left(t_f\right)-e_f\right]^2 \\ \left[i\left(t_f\right)-i_f\right]^2 \\ \left[\Omega\left(t_f\right)-\Omega_f\right]^2 \\ \left[\omega\left(t_f\right)-\omega_f\right]^2 \\ \left[f\left(t_f\right)-f_f\right]^2\end{cases} \tag{13}$$

Other formulations for the endpoint constraints can be used, but particular attention should be devoted to the order of magnitude of each component of the vectorial function.

Solution Strategy

The main problem in using orbital parameters as state representation of the dynamics is to deal with a stiff problem. The stiffness origins from the difference in the rate of variation of each orbital parameter. Indeed, while semi-major axis, eccentricity, inclination, RAAN and pericentre anomaly slightly change after the introduction of a perturbing acceleration, the true anomaly experiences a large variation in the same time window. This distinction leads to define the first group of orbital parameters as *slow variables*, while the true anomaly is denoted as *fast variable*. Moreover, it is possible to perform a further classification inside the category of the *slow variables* that is not reported because it does not affect the result. Two possible solutions have been considered in this paper for the solution of the stiff dynamical problem:

1. Integration of the differential equations considering a stiff numerical scheme.
2. Decomposition of the overall problem in two parts.

The first approach considers the use of a stiff numerical scheme for the solution of the differential equations. However, the DDP algorithm fails to converge whenever all the endpoint constraints are considered.

The second strategy splits the original problem in two parts. The first part considers the complete dynamics with only the endpoint constraints related to the slow variables. The second one considers the complete dynamics and all the endpoint constraints assuming as first guess the optimal solution obtained in the first previous part. This way the DDP algorithm converges to a solution. The analysis of the different behaviours suggests that the real problem is not the solver used for the resolution of the differential system, but the satisfaction of the constraint related to the fast variable together with the others.

The previous investigation discloses further considerations if the geometrical meaning of each orbital parameter is associated to the respective rate of variation. Semi-major axis, eccentricity, inclination, RAAN, and pericentre anomaly describes completely the orbit geometry and its position in the three-dimensional space. The true anomaly represents the position of the satellite on its orbit. Looking at Gauss' variational equations the presence of a term free from the disturbing accelerations in the true anomaly equation ensures that in a small time, the true anomaly changes faster than the other orbital elements. For each iteration of the DDP algorithm, the solution is corrected according to the magnitude of the difference between the exact final value of each orbital parameter and the actual one. The Lagrange multiplier variation related to the true anomaly will be so large to violate the assumption of linear-quadratic Taylor expansion causing the divergence in the next DDP iteration. From a physical point of view the DDP tries to optimise the trajectory so that the final true anomaly of the satellite is correct despite the correctness of the orbit geometry.

The organization of the overall optimisation process in two parts allows to obtain at the end of the first part an optimal solution with the final orbit geometry equal to the desired one, even if the satellite is not at the correct position. This represents already a preliminary good result that is not satisfactory in case rendezvous problems are considered. The use of this optimal solution as first guess for the overall optimisation problem restricts the search space in a region close to a quasi-optimal solution. However, for the same time length the variation related to the true anomaly is still higher than the other orbital parameters leading to the divergence of the problem. This problem is solved using a continuation technique for the true anomaly. The continuation technique consists in the achievement of the solution splitting the original problem in many subproblems where one parameter is gradually changed towards the desired value, and the solution for each subproblem is used as first guess for the next subproblem. This method is allowed because there are no constraints on the type of first guess solution that can be used. The continuation scheme is summarised in Figure 1.

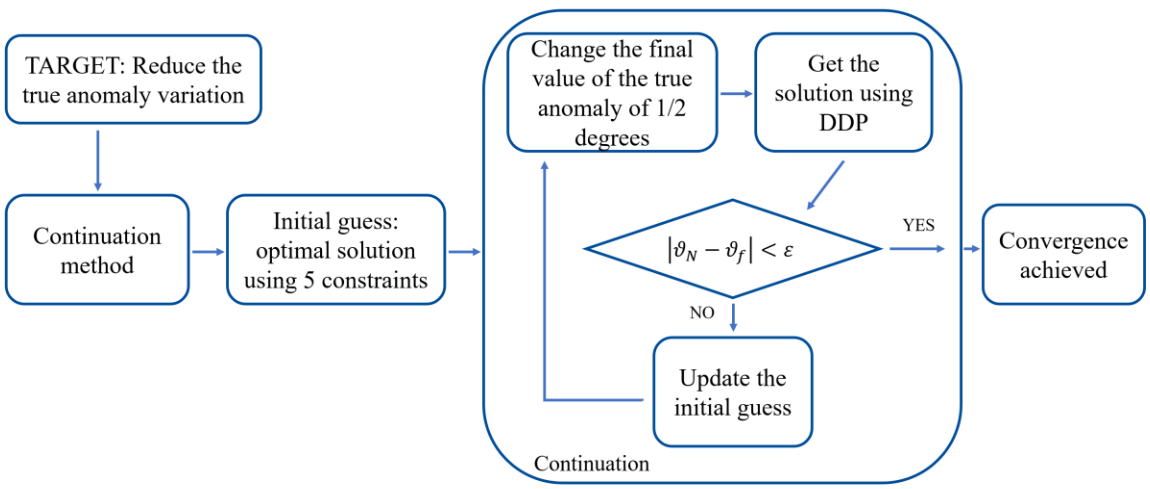

Figure 1. Continuation scheme.

From a physical point of view the decomposition of the overall problem in two parts constraints the DDP algorithm to construct in the first part the optimal trajectory to reach the final designed orbit, even if the final position is not the correct one. In the second part of the optimisation, the DDP is slightly adjusting the optimal trajectory used as first guess, so that the satellite is in the correct position at the final time. Thanks to the continuation technique the desired true anomaly is transformed into a vector of true anomalies from [f_i ,..., f_f], where f_i represent the true anomaly associated to the suboptimal solution of part one, and f_f is the desired final true anomaly. The consequence is that also the variation of the true anomaly becomes enough small to be consistent with the linear-quadratic expansion.

RESULTS

In this section the DDP algorithm is applied for solving three different orbit scenarios and check the effectiveness of the new proposed methodology:

1. Mars interplanetary transfer
2. Near-Earth asteroid transfer
3. Earth-satellite orbit raising

For each scenario, the same type of reference variables and set of tolerances is used. The numerical values are reported in Table 1.

Table 1. Tolerances and parameters for the DDP algorithm.

Parameter	Value
Tolerance for the first cycle	1e-6
Constraints tolerance	0.1 deg
n divisor	5

Mars interplanetary transfer

The first reference scenario considers an interplanetary transfer to Mars starting from the Earth. The initial conditions and final conditions for the problem are reported in Table 2 and Table 3.

Table 2. Initial data for Mars transfer.

Initial Data	Value
m_0	585 kg
Epoch	1234.5 MJD
TOF	200 days
Specific impulse, I_{sp}	4500 s
Nominal control	[0.0585,0,0]
Initial multipliers	$1e5 \cdot \varphi(\bar{\mathbf{x}}_f)$

Table 3. Mars final orbital parameters.

Final Parameters	Value
Semi-major axis	227940540.04 km
Eccentricity	0.0934
Inclination	1.85 deg
RAAN	49.59 deg
Pericentre anomaly	286.54 deg
True anomaly	100.21 deg

The initial guess for the control is a simple tangential thrust that is provided at each time step. The DDP algorithm is not constraining the initial guess used for the nominal control. It is obvious that the closer is the nominal control to the optimal solution, the lower is the computational time employed by the DDP algorithm to provide the optimal solution. In Figure 2 and Figure 3 the magnitude of the control law and the optimal control time history are shown, respectively.

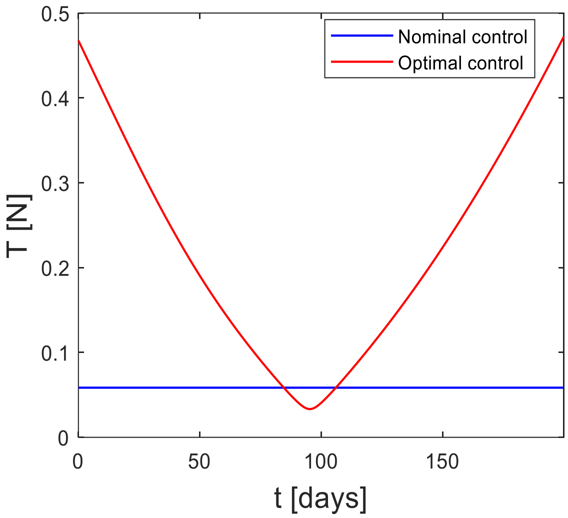

Figure 2. Magnitude of the control law.

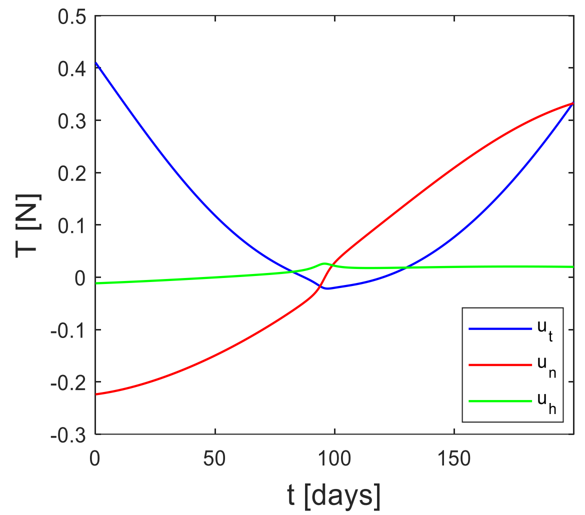

Figure 3. Optimal control law components.

The initial condition for the inclination has been set to a value slightly higher than zero to avoid the singularity embedded in the Gauss' dynamics in terms of classic Keplerian elements. The optimal trajectory given by the DDP algorithm for each orbital parameter is presented in Figure 4, Figure 5, Figure 6, Figure 7, Figure 8 and Figure 9.

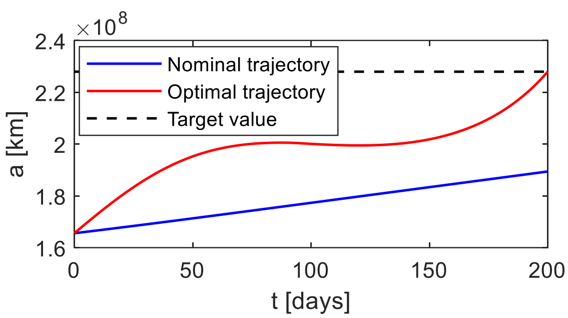

Figure 4. Semi-major axis time history.

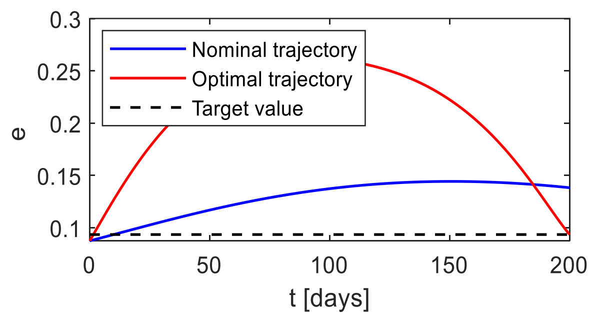

Figure 5. Eccentricity time history.

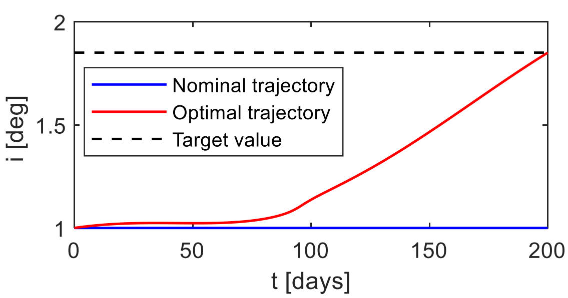

Figure 6. Inclination time history.

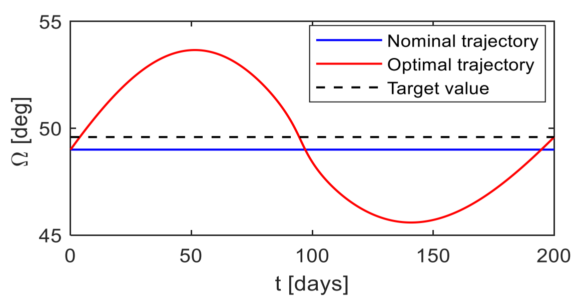

Figure 7. RAAN time history.

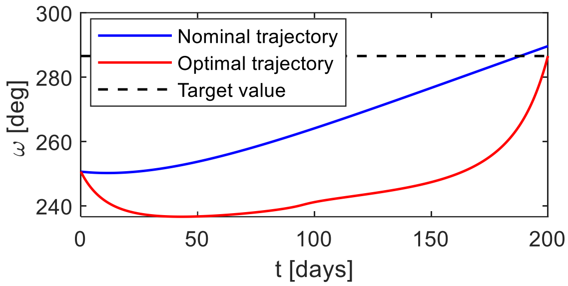

Figure 8. Pericentre anomaly time history.

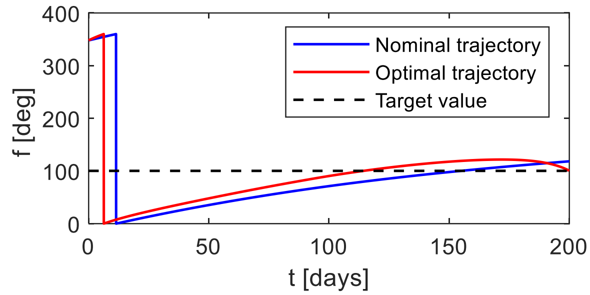

Figure 9. True anomaly time history.

Near-Earth Asteroid Transfer

The second example consists in an interplanetary transfer toward the near-Earth asteroid Apophis. The initial conditions and final conditions for the problem are reported in Table 4 and Table 5.

Table 4. Initial data for Apophis transfer.

Initial Data	Value
m_0	585 kg
Epoch	1234.5 MJD
TOF	200 days
Specific impulse, *Isp*	4500 s
Nominal control	[0.08,0,0]
Initial multipliers	$1e5 \cdot \varphi(\bar{\mathbf{x}}_f)$

Table 5. Apophis final orbital parameters.

Final Parameters	Value
Semi-major axis	190361131.76 km
Eccentricity	0.136534
Inclination	4.3777 deg
RAAN	104.41 deg
Pericentre anomaly	183.27 deg
True anomaly	322.53 deg

Also, in this case the initial guess for the control is set equal to a tangential control law to show that this simple nominal control can be used for different problems. The only constraint is to consider a magnitude such that in-plane orbital elements at the final time are close to the respective final values. In Figure 10 and Figure 11 the magnitude of the control law and the optimal control time history are shown, respectively.

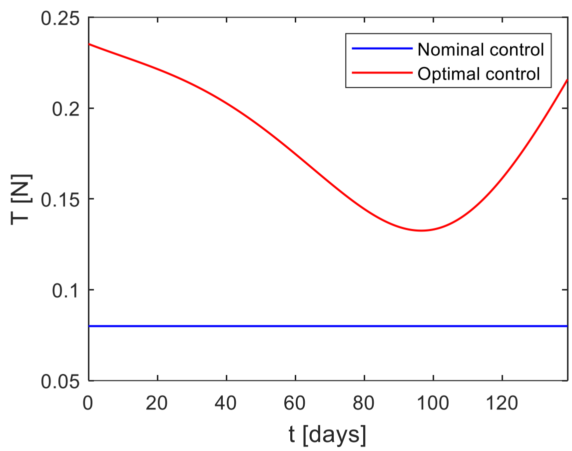

Figure 10. Magnitude of the control law.

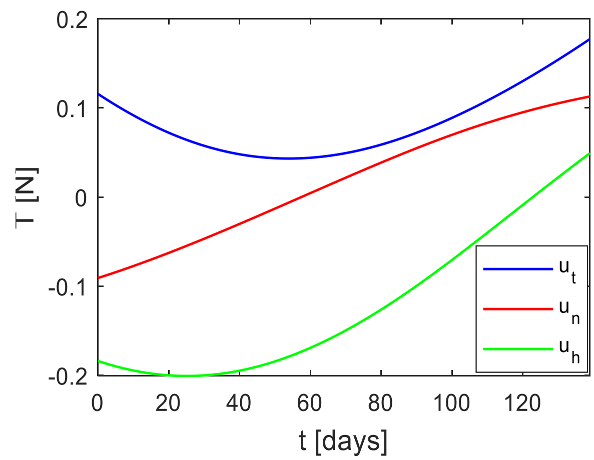

Figure 11. Optimal control law components.

This time the initial condition for the inclination has been set to zero because Gauss' equations in terms of modified equinoctial elements are used. The optimal trajectory given by the DDP algorithm for each orbital parameter is presented in Figure 12, Figure 13, Figure 14, Figure 15, Figure 16 and Figure 17. It is possible to check that the initial inclination is correctly set to zero looking at the initial condition of the equinoctial elements *h* and *k*.

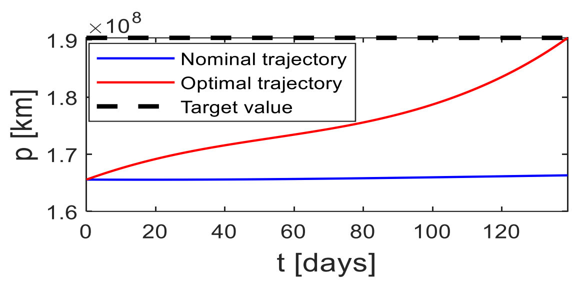

Figure 12. Semi-latus rectum time history.

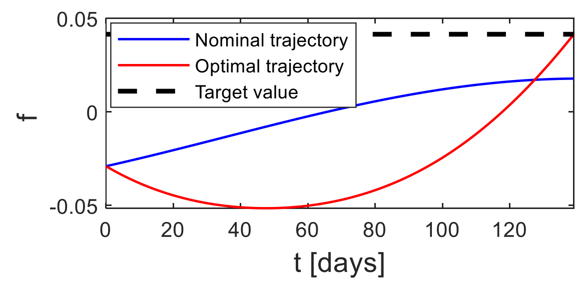

Figure 13. Time history of parameter *f*.

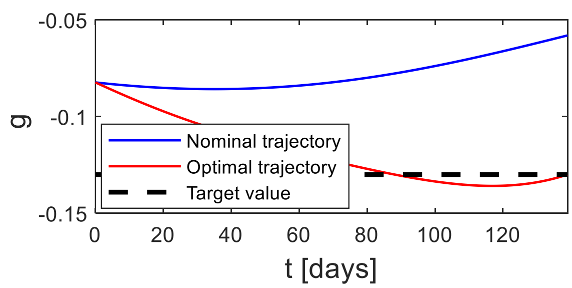

Figure 14. Time history of parameter *g*.

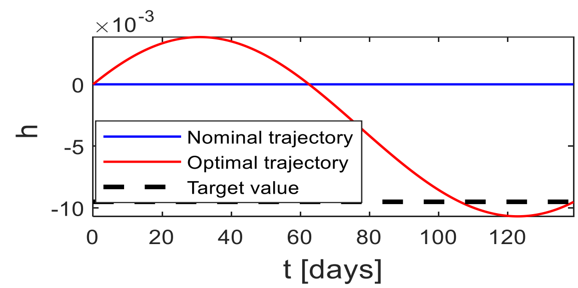

Figure 15. Time history of parameter *h*.

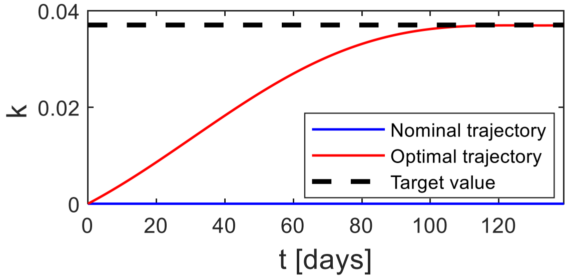

Figure 16. Time history of parameter *k*.

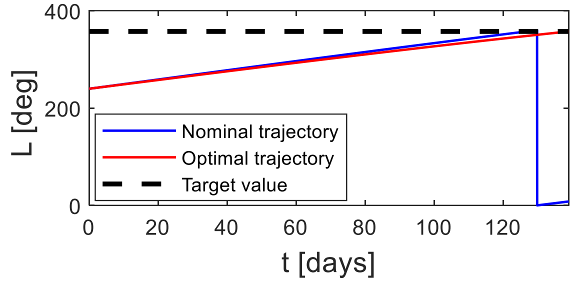

Figure 17. Ecliptic longitude time history.

Earth-satellite orbit raising

The last reference scenario considers an Earth-orbiting satellite performing an orbit raising manoeuvre. The initial conditions and final conditions for the problem are reported in Table 6 and Table 7.

Table 6. Satellite initial data.

Initial Data	Value
m_0	150 kg
Altitude	450 km
TOF	24 hours
Specific impulse, *Isp*	1500 s
Nominal control	[0.6,0,0]
Initial inclination	87.4 deg

Table 7. Final orbit parameters.

Final Parameters	Value
Altitude	1200 km
Eccentricity	0.05
Inclination	87.9 deg
RAAN	40 deg
Pericentre anomaly	40 deg
True anomaly	120 deg

In this case a planetary example is shown to check if the algorithm works also for orbits different from heliocentric orbits. The general behaviour is that the computational time increase because the Earth planetary constant that is used to compute the reference time is lower than the Sun gravitational parameter. Therefore, a higher number of time steps is necessary to get the same adimensional time step used for an interplanetary transfer.

Another important aspect analysed in this reference example is the possibility to include the effects of orbital perturbations in the DDP algorithm. Earth's oblateness through the first zonal harmonic J_2 is considered. The DDP algorithm is based on the analytical computation of the partials associated to the dynamics. If the expressions of the orbital perturbations are analytical, they can be inserted inside the equations of motions without changing the overall process.

In Figure 18 and Figure 19 the magnitude of the control law and the optimal control time history are shown, respectively considering a tangential control thrust as initial guess.

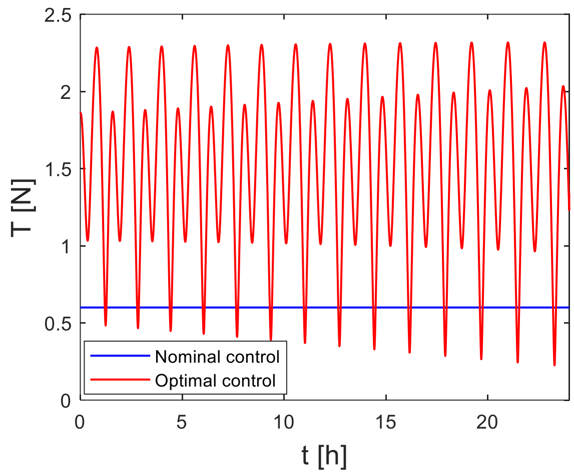

Figure 18. Magnitude of the control law.

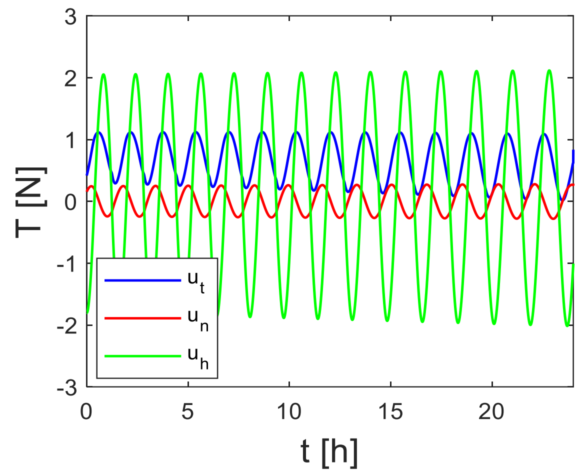

Figure 19. Optimal control law components.

The analytical expressions of J_2 perturbing accelerations in the radial-transversal-orthogonal reference frame is the following:[14]

$$
\begin{aligned}
a_{J_2 r} &= -\frac{3\mu J_2 R_{\oplus}^2}{2r^4}\left[1-3\sin^2 i \sin^2(\omega+f)\right] \\
a_{J_2 \theta} &= -\frac{3\mu J_2 R_{\oplus}^2}{2r^4}\sin^2 i \sin 2(\omega+f) \\
a_{J_2 h} &= -\frac{3\mu J_2 R_{\oplus}^2}{2r^4}\sin 2i \sin(\omega+f)
\end{aligned} \tag{14}
$$

The expressions of the disturbing accelerations must be rotated in the tangential-normal-orthogonal reference frame. The analytical formulations of the orbital perturbations increase the complexity of the dynamics. Therefore, also the partials evaluation computational time increases.

The optimal trajectory given by the DDP algorithm for each orbital parameter is presented in Figure 20, Figure 21, Figure 22, Figure 23, Figure 24 and Figure 25.

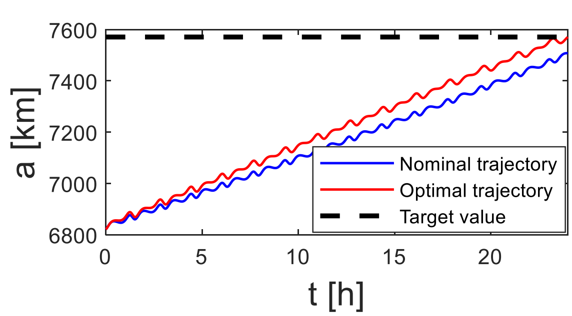

Figure 20. Semi-major axis time history.

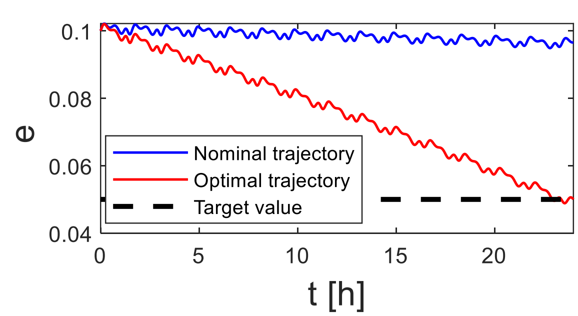

Figure 21. Eccentricity time history.

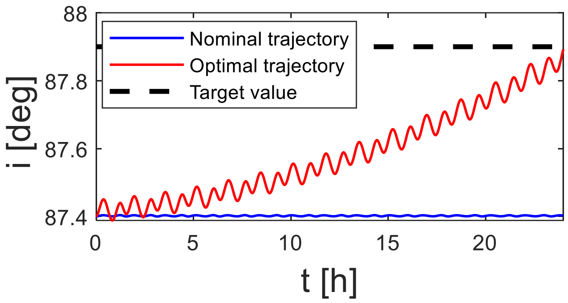

Figure 22. Inclination time history.

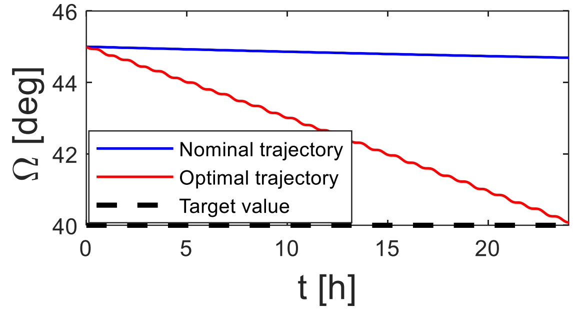

Figure 23. RAAN time history.

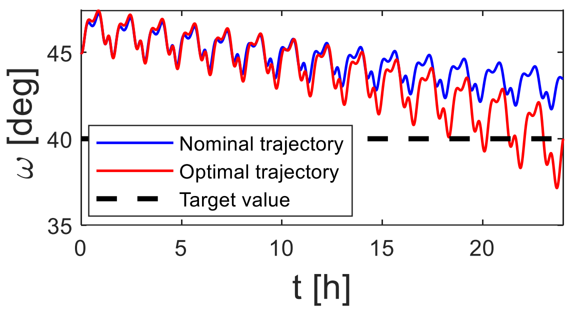

Figure 24. Pericentre anomaly time history.

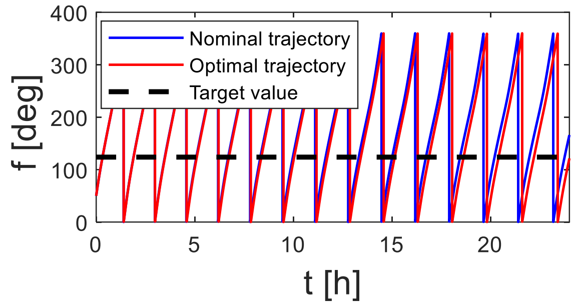

Figure 25. True anomaly time history.

The effect of J_2 orbital perturbation can be appreciated in the oscillations of the orbital elements given by the short-period variations that are not present in the previous two unperturbed examples.

CONCLUSION

In this paper a new methodology for solving the stiffness problem related to the application of the DDP algorithm to orbit dynamics expressed in terms of orbital elements is presented. After the adimensionalisation of the dynamics given by Gauss' variational equations and the endpoint constraints formulation, the minimum thrust problem has been solved thanks to the distinction between slow variables and fast variables. The continuation technique has been applied to achieve the convergence of the algorithm thanks to the splitting of the overall problem in many subproblems. The new methodology has been applied considering both classic Keplerian elements and modified equinoctial elements for a Mars interplanetary trajectory, near-Earth asteroid transfer and an Earth-satellite orbit raising. The algorithm converges without the application of the continuation technique removing the fast variable. This result suggests to investigate the application of the DDP to the averaged dynamics using semi-analytical techniques.

ACKNOWLEDGMENTS

The research leading to these results has received funding from the European Research Council (ERC) under the European Union's Horizon 2020 research and innovation program as part of project COMPASS (Grant agreement No 679086).

REFERENCES

[1] M. La Mantia and L. Casalino, "Indirect optimization of Low-Thrust Capture Trajectories", *Journal of Guidance, Dynamic, and Control,* Vol. 29, No. 4, 2016, pp. 1011-1014.

[2] J.B. Betts, "Very low-thrust trajectory optimization using a direct SQP method", *Journal of Computation and Applied Mathematics,* Vol. 120, Issue 1-2, 2000, pp. 27-40.

[3] D.H. Jacobson and D.Q. Mayne, *Differential Dynamic Programming,* American Elsevier Publishing Company, 1970.

[4] S.B. Gershwin and D.H. Jacobson, "A discrete-time differential dynamic programming algorithm with application to optimal orbit transfer", *AIAA Journal*, Vol. 8, No. 9, 1970, pp. 1616-1626.

[5] F.A. El-Awar, J.W. Labadie and T.B.M.J. Ouarda, Stochastic differential dynamics programming for multi-reservoir system control, *Stochastic Hydrology and Hydraulics,* Vol. 12, 1998, pp. 247-266.

[6] C.A. Shoemaker and G.J. Whiffen, "Feedback control of groundwater remediation", *Patent Number 5468088*, 1995.

[7] G.J. Whiffen, "Mystic: Implementation of the Static Dynamic Optimal Control Algorithm for High-Fidelity Low-Thrust Trajectory Design", *AIAA/AAS Astrodynamics Specialist Conference and Exhibit,* 2006.

[8] C. Colombo, M. Vasile and G. Radice, "Optimal low-thrust trajectories to asteroids through an algorithm based on differential dynamic programming", *Celestial Mechanics and Dynamical Astronomy,* Vol. 105, 2009, pp. 75-112.

[9] G. Lantoine and R.P. Russell, "A Hybrid Differential Dynamics Programming Algorithm for Constrained Optimal Control Problems. Part 1: Theory", *Journal of Optimization Theory and Applications,* Vol. 154, 2012, pp. 382-417.

[10] N. Ozaki, S. Campagnola, R. Funase and C.H. Yam, "Stochastic Differential Dynamics Programming with Unscented Transform for Low-Thrust Trajectory Design", *Journal of Guidance, Control, and Dynamics,* Vol. 41, No. 2, 2018, pp. 377-387.

[11] R. Bellman, *Dynamic Programming*, Princeton University Press,1957.

[12] R.H. Battin, *An Introduction to the Mathematics and Methods of Astrodynamics*, AIAA Educational Series, 1999.

[13] E.A. Roth, "The Gaussian form of the variation-of-parameter equations formulated in equinoctial elements-Applications: airdrag and radiation pressure", *Acta Astronautica,* Vol. 12, No. 10, 1985, pp. 719-730.

[14] H.D. Curtis, *Orbital Mechanics for Engineering Students*, Third Edition, Elsevier Aerospace Engineering Series, 2014.